International Journal of Electrical Components and Energy Conversion
2021; 7(2): 42-47
http://www.sciencepublishinggroup.com/j/ijecec
doi: 10.11648/j.ijecec.20210702.12
ISSN: 2469-8040 (Print); ISSN: 2469-8059 (Online)

Minimization of the Electromagnetic Torque Ripple of a Synchronous Reluctance Generator Using External Rotor Excitation

Jesus Gonzalez*, Concepcion Hernandez, Marco Arjona

Graduate and Research Center, National Technology Institute of Mexico Campus La Laguna, Torreon, Mexico

Email address:
jesus.gonzalez.itl@outlook.com (J. Gonzalez)

*Corresponding author

To cite this article:
Jesus Gonzalez, Concepcion Hernandez, Marco Arjona. Minimization of the Electromagnetic Torque Ripple of a Synchronous Reluctance Generator Using External Rotor Excitation. *International Journal of Electrical Components and Energy Conversion.* Vol. 7, No. 2, 2021, pp. 42-47. doi: 10.11648/j.ijecec.20210702.12

Received: September 10, 2021; **Accepted**: October 5, 2021; **Published**: October 15, 2021

Abstract: This paper presents an approach to minimize the electromagnetic torque ripple of a synchronous reluctance generator (SynRG) with a magnetic field created by externally excited rotor coils. The synchronous reluctance machine is widely used in low and medium power systems such as wind power generation and new electric vehicle technologies. This paper proposes a rotor topology with flux barriers and direct current excited coils that reduce the torque ripple and replace the permanent magnets used in other reluctance rotor topologies. First, the initial rotor design, without excitation coils, is optimized to obtain a new rotor structure that reduces the electromagnetic torque ripple. In this work, the optimization of the rotor geometry was achieved by using genetic algorithms and the finite element method to optimize and parameterize the main components of the machine. In the optimized rotor model, an external electronic converter is included to feed the coils positioned between the magnetic flux barriers and the segments formed by the ferromagnetic material of the rotor. Finally, the electrical and magnetic machine variables obtained from implementing the coils into the optimized rotor are compared to the initial rotor structure operating under nominal load conditions to demonstrate the advantage of this topology in minimizing the electromagnetic torque ripple.

Keywords: Externally Excited Coils, Optimized Rotor, Synchronous Reluctance Generator

1. Introduction

With the advances in power electronics, synchronous reluctance machines have been part of numerous investigations in recent years. This is due to the advantages they offer compared to other types of rotating machines, thereby achieving greater acceptance in different areas of the energy sector. However, due to the complicated manufacturing process and high cost of permanent magnets, this work analyzes the implementation of coils with external excitation that power electronics can regulate. Furthermore, the radial structure and ferromagnetic material allow a higher magnetic flux saturation in the bridges (rotor parts that link one segment to another), creating magnetic poles in the rotor.

Different rotor topologies and configurations for synchronous reluctance machines have the common objective of mitigating the electromagnetic torque ripple to avoid mechanical vibrations affecting machine performance.

In *Polyphase reaction synchronous motors* [1] is presented the theory and principles of operation of this type of rotor used in polyphase machines, comparing it with the behavior of induction machines, and different rotor structures are analyzed. In *Torque ripple minimization in synchronous reluctance motor using a sinusoidal rotor lamination shape* [2] and *Improvement of Torque Characteristics For a Synchronous Reluctance Motor Using MMA-based Topology Optimization Method* [3], the improvement of the electromagnetic torque ripple is discussed by varying the shape of the axial and radial laminations of the rotor, respectively. In *Effect of Rotor Geometry on Peak and Average Torque of External-Rotor Synchronous Reluctance Motor in Comparison With Switched Reluctance Motor for*

Low- Speed Direct-Drive Domestic Application [4], different models are developed for an external reluctance rotor by varying the size and shape of the ribs to achieve a reduction in the electromagnetic torque ripple. In *The Design and Optimization of an Interior, Permanent Magnet Synchronous Machine Applied in an Electric Traction Vehicle Requiring a Low Torque Ripple* [5], the optimization of the rotor of a reluctance machine with permanent magnets is presented considering different parameters such as the rotor surface, the positioning of the permanent magnets, and the iron bridges to improve the ripple of the electromagnetic torque. In *Design and Analysis of Two Permanent-Magnet-Assisted Bearingless Synchronous Reluctance Motors with Different Rotor Structure* [6], two types of rotors with inserted permanent magnets but different magnetic barrier structures are implemented. The advantages of each design are explained, including the improvements in average torque, power factor, and electromagnetic torque ripple.

The main disadvantages of using permanent magnets, such as irreversible demagnetization, which causes poor performance in this machine, are detailed in *Multi-Objective Optimization of Permanent Magnet Synchronous Motor for Electric Vehicle Considering Demagnetization* [7]. In addition, *Detection of Eccentricity Faults in Five Phase Ferrite PM Assisted Synchronous Reluctance Machines* [8] discusses the failures due to eccentricities in the rotor with inserted permanent magnets, leading to the generation of mechanical stress and electromagnetic asymmetries, which worsens the machine performance. The topology of a hybrid rotor model with permanent magnets and excitation coils is analyzed in *Analysis of Magnetic Field and Electromagnetic Performance of a New Hybrid Excitation Synchronous Motor with dual-V type Magnets* [9]. The advantages are also shown, such as improving the airgap flux density. A topology with excitation in the rotor that can be suitable for generator/motor used in automobiles is reported in *BEGA-a biaxial excitation Generator for automobiles: comprehensive characterization and test results* [10]; this type of topology with coils in the rotor can also be implemented as a generator for different applications detailed in *Design and performance of compensated reluctance synchronous machine drive with extended constant power speed range* [11] and *Electromagnetic analysis of a wound-field generator with flux-barrier rotor for AC generator sets* [12]. In *Reluctance synchronous wind generator design optimisation in the megawatt, medium speed range* [13], a different coil configuration on the rotor is implemented in wind energy conversion systems in medium speed ranges. Finally, in *Genetic algorithms in design of a synchronous reluctance motor* [14], genetic algorithms (GA) are used to optimize the rotor structure of a synchronous reluctance motor from its basic un-predetermined geometry.

The main objective of this work is to achieve the minimization of the electromagnetic torque ripple with the implementation of external rotor excitation in a SynRG. The first step is to optimize the structure of a variable reluctance rotor through genetic algorithms, to incorporate later external excitation coils arranged differently and with a different rotor structure from those mentioned in the previous bibliography. Then, the electromagnetic analysis of the proposed topology is presented. Finally, the electromagnetic variables of the three models are compared: the initial rotor structure, the optimized structure, and the optimized structure with the externally excited coils. As a result, a considerable improvement of the electromagnetic torque ripple was achieved.

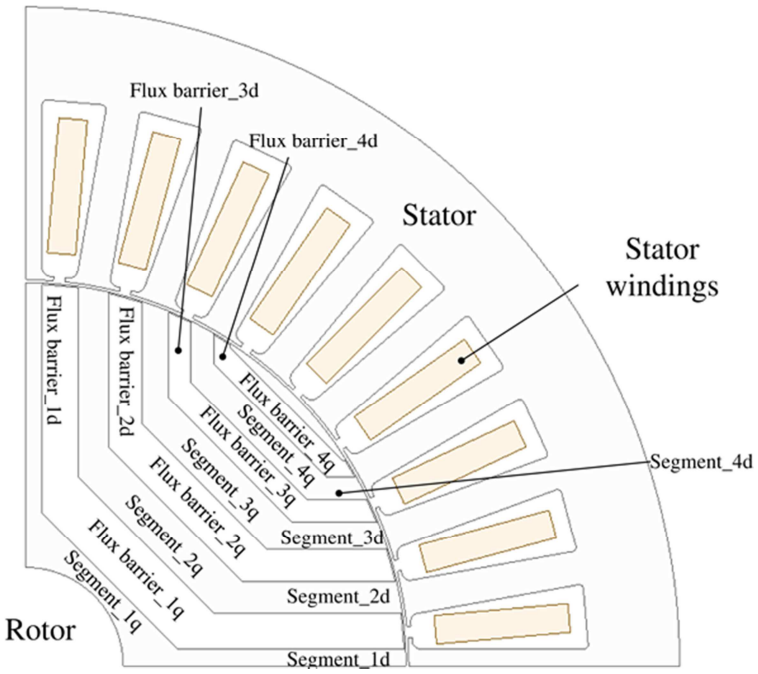

Figure 1. *Cross-section of the SynRG.*

2. SynRG Main Dimensions

The initial rotor design of the synchronous reluctance machine was based on the theory established in *Synchronous Reluctance Machine (SynRM) Design* [15], *Novel High-Performance SynRM Design Method: An Easy Approach for A Complicated Rotor Topology* [16], *Design Optimization and Performance Improvement of Synchronous Reluctance Machines which consists of sizing and positioning the flux barriers in the rotor* [17] and *Comprehensive Design Procedure and Manufacturing of Permanent Magnet Assisted Synchronous Reluctance Motor* [18]. Figure 1 shows the main components of the SynRG, such as the stator core, the windings, and the rotor formed by the magnetic flux barriers and segments in the d-q axes.

Table 1 shows the dimension and parameters of the machine, and whose primary values are calculated by using the equations described in *Reluctance Synchronous Machines and Drives* [19] and). *Design of rotating electrical machines* [20]. Once these values are obtained, they are parameterized in the finite element model to create a first rotor structure [21].

Table 1. *Design data of the SynRG*

Description	Unit	Value
Power	W	900
Voltage	V	220
Speed	r.p.m	900
Poles	---	4
Lamination Type	---	M22-24G
Stator length	mm	73.95
Inner stator diameter	mm	94.15
Outer stator diameter	mm	160.69
Stator tooth width	mm	4.16
Slot height	mm	20
Stator slot opening	mm	2.2
Slots	---	36
Number of turns/phase	---	108
Rotor diameter	mm	93.46
Shaft diameter	mm	24

3. Optimization Methodology

The first step in optimizing the initial designed rotor of the SynRG is to define an objective function and solve it with genetic algorithms [22]. The cost function is defined as the minimization of the electromagnetic torque ripple, as indicated by (1) [17].

$$Min\ T_{ripple}(x) = \left(T_{max}(x) - T_{min}(x)\right)/T_{average}\,(x) \quad (1)$$

s.t.

$$x_{min} \leq x \leq x_{max}$$

where T_{max} is the maximum electromagnetic torque, T_{min} is the minimum electromagnetic torque, and $T_{average}$ is the average electromagnetic torque obtained; $\boldsymbol{x}$ is the design variable vector indicated in Table 2, and it corresponds to the segments and the rotor flux barriers widths in the d-q axes. The subscripts max and min indicate the maximum and minimum bounds, respectively. The maximum values were established as the total amount of material and air (total sum of segments and flux barriers widths) of the initial rotor along the d-q axes.

The objective of this method, based on the equation described above, is to modify the initial rotor dimensions so that the ripple of the electromagnetic torque decreases to incorporate the external excitation coils later. The design procedure can be observed in the flowchart shown in Figure 2. As mentioned in *Synchronous Reluctance Machine (SynRM) Design* and *Design Optimization and Performance Improvement of Synchronous Reluctance Machines* [15, 17], an improved machine performance is achieved by varying these rotor variables. Furthermore, the computation time of the rotor optimization calculations was reduced by modeling a quarter of the total geometry of the SynRG, taking advantage of the periodicity boundary condition of the electrical machine.

In this work, the genetic algorithm optimizer used in the finite element software was tuned with the following parameters: a maximum number of 20 generations, parents: 20, crossover type: simulated binary crossover, individual crossover probability: 1, mutation type: polynomial mutation, individual mutation probability: 1, children and survivals from Pareto front: 20, which resulted in 400 iterations to obtain the optimized rotor variable values shown in Table 2.

Once the initial rotor structure has been optimized, by using the new dimensions, a new rotor structure is modified in the q axis, resulting in a rotor structure, as it is shown in Figure 3 (c). Finally, to carry out the electromagnetic analysis, a 2D finite element transient solver was used. Different scenarios of nominal operating conditions were simulated to compare the electromagnetic output variables of the three models where the identical stator dimensions were used in all cases.

Table 2. *Design variables of the rotor.*

Design variables	Initial rotor values (mm)	Min values (mm)	Max values (mm)	Optimal values (mm)
Segment_1d	2.2494	1.9300	2.2500	2.0638
Segment_2d	4.3108	3.6860	4.3110	3.7318
Segment_3d	3.7625	3.1750	3.7630	3.1909
Segment_4d	2.8998	2.3770	2.9040	2.7402
Flux barrier_1d	5.0950	4.3540	5.0950	4.5237
Flux barrier_2d	4.2790	3.5990	4.2790	3.6526
Flux barrier_3d	2.9139	2.3570	2.9140	2.3890
Flux barrier_4d	2.2043	1.4600	2.2043	1.8193
Segment_1q	2.7526	2.5100	2.7530	2.6491

Design variables	Initial rotor values (mm)	Min values (mm)	Max values (mm)	Optimal values (mm)
Segment_2q	5.2678	4.8845	5.2680	5.2003
Segment_3q	4.5759	4.4970	4.8590	4.5637
Segment_4q	3.4894	3.4890	3.8450	3.6282
Flux barrier_1q	6.2890	4.4520	6.2890	4.7438
Flux barrier_2q	5.2508	3.9850	5.2510	4.2164
Flux barrier_3q	3.5249	3.1510	3.5250	3.2003
Flux barrier_4q	2.4750	2.4750	5.9510	3.5419

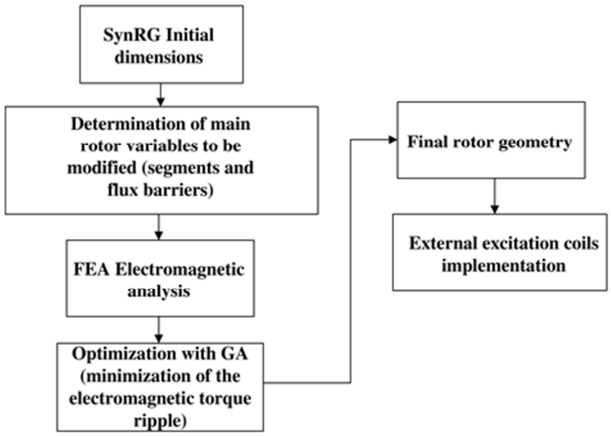

Figure 2. *Design methodology.*

4. Electromagnetic Analysis

4.1. Rotor with DC External Excitation Configuration

Figure 4 shows the configuration of the coils in the rotor, the external circuit, and the equivalent circuit of the stator coils connected to a balanced resistive load, with a value of 11 Ohm per phase.

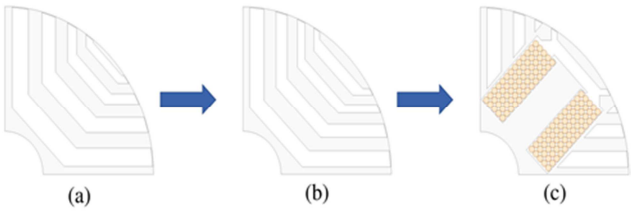

Figure 3. *Structures of the (a) Initial rotor, (b) Optimized rotor, and (c) Rotor with external excitation coils.*

The external circuit configuration that feeds the excitation coils is a well-known and established configuration. A co-simulation is performed between a permanent magnet synchronous generator and a three-phase diode rectifier [23]. However, in this work, the main objective of the electronic power circuit employs an external sinusoidal three-phase source connected to a diode bridge that rectifies the voltage signal and feeds the coil with the polarity shown in Figure 5. It can also be seen every single conductor's characterization to obtain a more detailed model.

The number of turns and the excitation current is defined based on the limitations described in *Optimum Design of an Extended Range Generator for EVs Based on Taguchi Method* [24]. Based on these limitations, 65 turns and a current of 25 A were employed, the cross-section of each conductor which is 2.58 mm² and the available area between the flux barriers and the rotor segments were taken into account. The rotor is the component of main interest to be analyzed; hence it was decided not to characterize the stator conductors in too much detail because this would significantly increase the computation time.

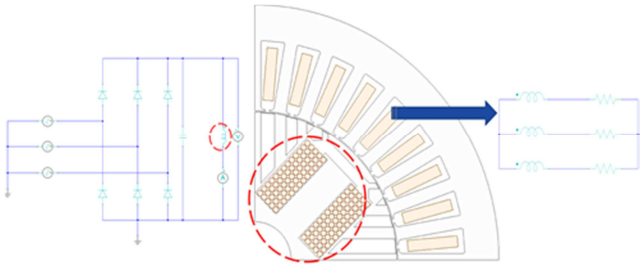

Figure 4. *Rotor and stator equivalent circuits configuration.*

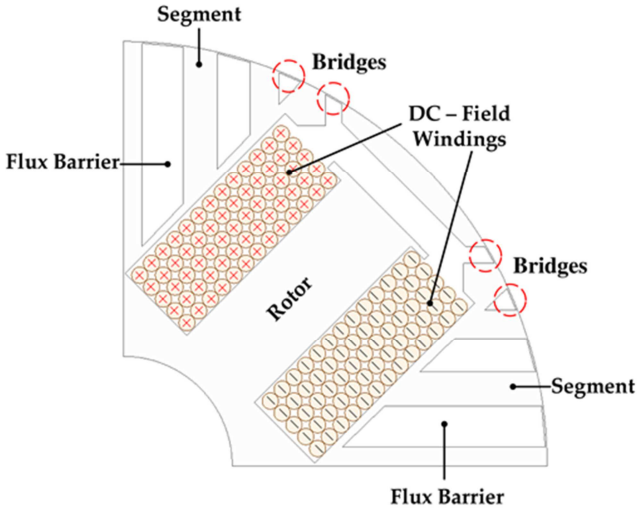

Figure 5. *Rotor winding configuration.*

4.2. Rotor with DC External Excitation Results

Figure 6 illustrates the magnetic flux lines created when the electronic converter feeds the external excitation coil, and the stator is without load. Figure 7 shows the magnetic flux density in the direct current excited rotor machine operating at nominal conditions.

It is clearly seen that the most significant magnetic saturation is located in the parts of the rotor close to the excitation coils. The induced voltages and currents in the stator generator terminals are shown in figures 8 and 9, respectively.

Figure 10 shows the comparison of the electromagnetic torque ripple waveform in the three analyzed topologies, a

decrease in ripple is seen in the first optimized rotor model with respect to the initial model, as well as a decrease in the optimized model with the external excitation coils compared to the initial model. Table 3 shows the numerical comparison, where a reduction in the ripple of the electromagnetic torque of 65% is observed, comparing the original rotor structure with respect to the topology proposed with the external excitation coils.

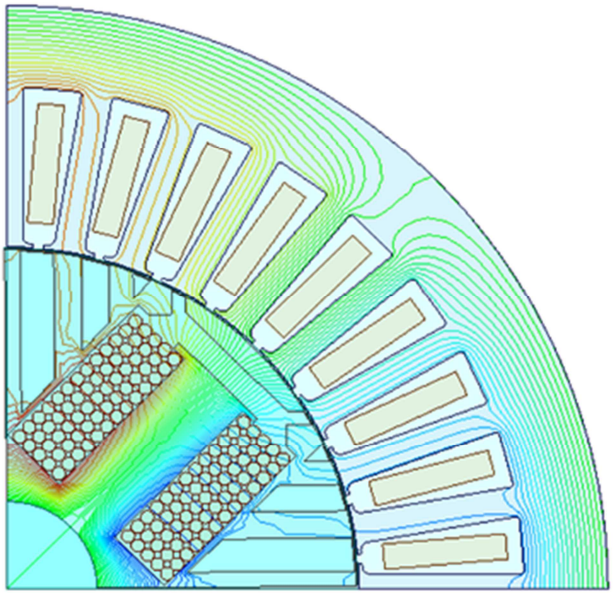

Figure 6. *Magnetic flux lines produced by the DC excited coils.*

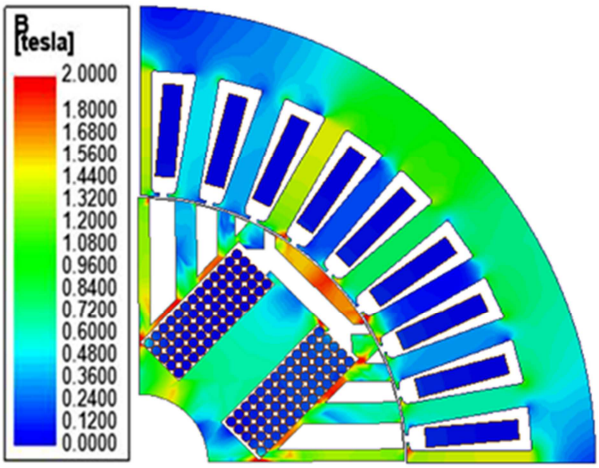

Figure 7. *Magnetic flux density in the DC excited rotor.*

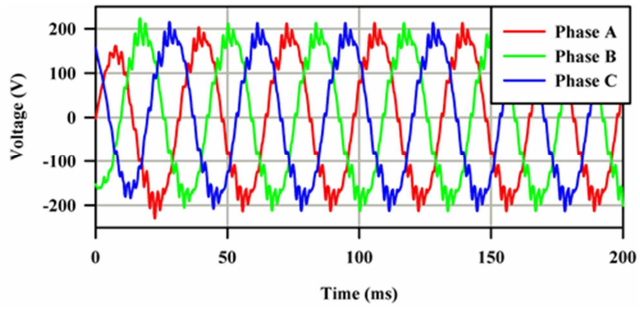

Figure 8. *Induced voltages in the stator terminals.*

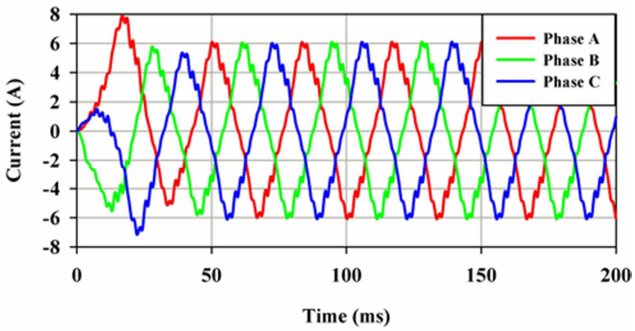

Figure 9. *Currents in the stator terminals.*

Figure 11 illustrates the magnetic flux densities in the three different rotor models when the SynRG is operating under nominal load conditions; it can be seen how the magnetic flux density increases in the rotor parts near to the airgap due to the field created by the externally excited coils. The analysis of the magnetic field distribution in this region is an important aspect to consider since this is the place where the conversion of mechanical into electrical energy takes place.

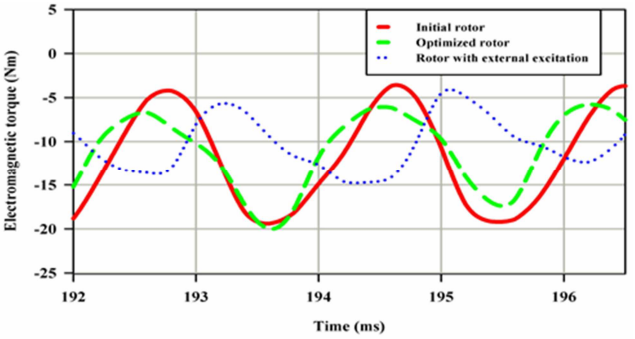

Figure 10. *Electromagnetic torque comparison.*

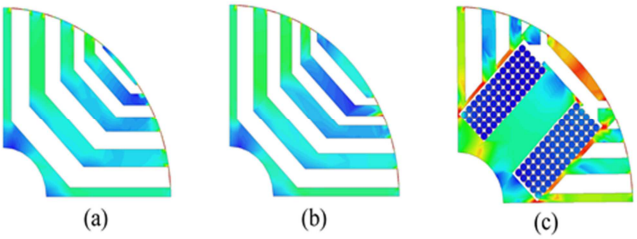

Figure 11. *Magnetic flux densities in the (a) Initial rotor, (b) Optimized rotor, and (c) Rotor with external excitation coils.*

Table 3. *Electromagnetic torque ripple numerical comparison.*

Rotor structure	T_{max} (Nm)	T_{min} (Nm)	$T_{average}$ (Nm)	% T_{ripple}
Initial Rotor	-19.3	-3.6	-12	131%
Optimized Rotor	-20	-5.7	-12	118%
Rotor with external excitation coils	-12.3	-4.4	-12	65%

5. Conclusions

In this work, genetic algorithms were used to obtain a rotor structure that reduces the ripple of the electromagnetic torque, first without excitation and then incorporating excitation coils between the flux barriers and segments in the optimized

rotor structure. The comparison of the different rotor models was made to demonstrate the advantage offered by implementing the excitation in the rotor, achieving a considerable reduction in the percentage of the electromagnetic torque ripple, which is desirable for a good performance in this type of machine. Furthermore, the coil excitation approach is considered attractive when the cost or availability of permanent magnets represents a constraint in different synchronous reluctance machine applications in electrical systems. As future work, the implementation of the circuit that feeds the external coils can be carried out in the Simplorer software to replace the diodes with igbts that can be controlled through a co-simulation with Simulink.

Acknowledgements

The authors wish to thank the Energy Sustainability CONACYT-SENER Fund, INEEL, CONACYT, Tecnológico Nacional de México, and Instituto Tecnológico de la Laguna for the financial support under grant No. 206842-P10 to carry out this research.

References

[1] Kostko, J. K. (1923). Polyphase reaction synchronous motors. Journal of the American Institute of Electrical Engineers, 42 (11): 1162-1168.

[2] Muteba, M., Twala, B., & Nicolae, D. V. (2016). Torque ripple minimization in synchronous reluctance motor using a sinusoidal rotor lamination shape, XXII IEEE International Conference on Electrical Machines (ICEM), 606-611.

[3] Okamoto, Y., Hoshino, R., Wakao, S., & Tsuburaya, T. (2018). Improvement of Torque Characteristics For a Synchronous Reluctance Motor Using MMA-based Topology Optimization Method, IEEE Transactions on Magnetics, 54 (3): 1–4.

[4] Raj, M. A., & Kavitha, A. (2017). Effect of Rotor Geometry on Peak and Average Torque of External-Rotor Synchronous Reluctance Motor in Comparison With Switched Reluctance Motor for Low- Speed Direct-Drive Domestic Application, IEEE Transactions on Magnetics, 53 (11): 1–8.

[5] Zhang, G., Yu, W., Hua, W., Cao, R., Qiu, H., & Guo, A. (2019). The Design and Optimization of an Interior, Permanent Magnet Synchronous Machine Applied in an Electric Traction Vehicle Requiring a Low Torque Ripple. Applied Sciences, 9, 3634.

[6] Hua, Y., Zhu, H., Gao, M., & Ji, Z. (2021). Design and Analysis of Two Permanent-Magnet-Assisted Bearingless Synchronous Reluctance Motors with Different Rotor Structure. Energies, 14, 879.

[7] You, Y., & Yoon, K. (2021). Multi-Objective Optimization of Permanent Magnet Synchronous Motor for Electric Vehicle Considering Demagnetization. Applied Sciences, 11, 2159.

[8] López-Torres, C., Riba, J. R., Garcia, A., & Romeral, L. (2017). Detection of Eccentricity Faults in Five Phase Ferrite PM Assisted Synchronous Reluctance Machines. Applied Sciences. 7, 565.

[9] Hu, W., Zhang, X., Yin, H., Geng, H., Zhang, Y., & Shi, L. (2020). Analysis of Magnetic Field and Electromagnetic Performance of a New Hybrid Excitation Synchronous Motor with dual-V type Magnets. Energies. 13, 1501.

[10] Scridon, S., Boldea, I., Tutelea, L., Blaabjerg, F., & Ritchie, A. E. (2005). BEGA-a biaxial excitation Generator for automobiles: comprehensive characterization and test results. IEEE Transactions on Industry Applications. 41 (4): 935-944.

[11] Kamper, M. J., & Villet, W. T. (2012). Design and performance of compensated reluctance synchronous machine drive with extended constant power speed range. IEEE Energy Conversion Congress and Exposition (ECCE). 4330-4337.

[12] Fernandez, S. A., Prieto, D., Vannier, J., Manfe, P., & Saint-Michel, J. (2015). Electromagnetic analysis of a wound-field generator with flux-barrier rotor for AC generator sets. IEEE International Electric Machines & Drives Conference (IEMDC). 273-279.

[13] Howard, E., & Kamper, M. J. (2017) Reluctance synchronous wind generator design optimisation in the megawatt, medium speed range. IEEE Energy Conversion Congress and Exposition (ECCE). 1864-1871.

[14] Zagirnyak, M. V., Maga, D., & Miljavec, D. (2011). Genetic algorithms in design of a synchronous reluctance motor. 14th International Conference Mechatronika. 25-30.

[15] Moghaddam, R. R. (2007). Synchronous Reluctance Machine (SynRM) Design. M. Sc. dissertation, Dept. Elect. Eng., Royal Inst. Of Tech., Stockholm, Sweden.

[16] Moghaddam, R., & Gyllensten, F. (2014). Novel High-Performance SynRM Design Method: An Easy Approach for A Complicated Rotor Topology. IEEE Trans. Ind. Electron. 61 (9): 5058-5065.

[17] Abeyrathne, I, P. (2019). Design Optimization and Performance Improvement of Synchronous Reluctance Machines. Dept. Elect. And Computer. Eng. University of Manitoba, Winnipeg, Canada.

[18] Aghazadeh, H., Afjei, E., & Siadatan, A. (2019). Comprehensive Design Procedure and Manufacturing of Permanent Magnet Assisted Synchronous Reluctance Motor. IJE TRANSACTIONS C. 32 (9): 1299-1305.

[19] Boldea, I. (1996). Reluctance Synchronous Machines and Drives. Clarendon Press.

[20] Pyrhönen, J., Jokinen, T., & Hrabovkowá, V. (2014). Design of rotating electrical machines. Second edition ed: Wiley.

[21] ANSYS, Maxwell User Manual. (2020).

[22] Kramer, O. (2017) Genetic Algorithm Essentials. Springer.

[23] Quintal-Palomo, R. E., Gwozdziewicz, M., & Dybkowski, M. (2019). Modelling and co-simulation of a permanent magnet synchronous generator. COMPEL - The international journal for computation and mathematics in electrical and electronic engineering. 38 (6): 1904-1917.

[24] Yao, S., & Zhang, W. (2018). Optimum Design of an Extended Range Generator for EVs Based on Taguchi Method. IEEE Student Conference on Electric Machines and Systems. 1-6.